Electronic Supplementary information for

Observation of wrapping mechanism in amine carbon dioxide molecular interactions on heterogeneous sorbents

Damien Thirion[1], Vepa Rozyyev[2], Joonho Park[1], Jeehye Byun[1], Yousung Jung[1], Mert Atilhan[3], Cafer T. Yavuz[1,2]*

[1]Graduate School of EEWS, and[2]Department of Chemistry, KAIST, Daejeon, 305-701 Korea, yavuz@kaist.ac.kr
[3]Department of Chemical Engineering, Qatar University, Doha, Qatar

Content

- **FIGURE S12: SEM IMAGES OF COP-115 (TOP), COP-115-A (MIDDLE) AND COP-115-B (DOWN) AT 1 ΜM (LEFT) AND 400 NM (RIGHT) MAGNIFICATION.**

MATERIALS AND METHOD

4,4'-bis-(chloromethyl)-1,1'-biphenyl was obtained from TCI, Japan, methanesulfonic acid from Sigma-Aldrich, USA and other chemicals and solvents from Samchun Pure Chemicals, Korea and used without further purification unless otherwise specified. Dichloroethane was distilled over P_2O_5 under argon prior to use. Elemental analyses were performed at the KAIST Central Research Instrument Facility on a Thermo Scientific FLASH 2000 equipped with a TCD detector. Solid-state ^{13}C cross-polarization magic angle spinning NMR (CP-MAS) was performed at the KAIST Central Research Instrument Facility on an Agilent 400 MHz 54mm DD2 equipped with a HFXY 1.6 mm probe. The contact time was 5ms with a delay of 3 s. All samples were spun at 15 kHz. Infrared spectra (FT-IR) were recorded at KAIST energy and environment research center with a Jasco FT/IR-4100 type-A spectrometer using KBr pellets. In-situ difference infrared spectra of adsorbed CO_2 were recorded on an Agilent Cary 660 FTIR with a diffuse reflectance cell connected to gas lines. COP-115-C samples were degassed in N_2 at 150°C for 5 hours and used as background before switching to CO_2 flow. Spectra were recorded until stable and reflect the absorbed CO_2 on the sample. Thermogravimetric analyses were performed on a Shimadzu DTG-60A by heating the samples up to 800 °C at a rate of 10 °C min^{-1} under nitrogen or air atmosphere. Textural characterization of polymers was carried out from nitrogen adsorption isotherms using a Micromeritics 3FLEX accelerated surface area and porosimetry analyzer at 77 K. Prior to measurement, samples were degassed at 423 K for 5 h under vacuum. The specific surface areas were derived from Brunauer-Emmett-Teller (BET) method. Pore size distribution was calculated with the Micromeritics 3FLEX software using a single-walled carbon nanotube DFT model with cylindrical pores. This model was chosen as it gave the best fit between experiment and calculation. Isosteric heats of adsorption were calculated from CO_2 adsorption isotherms up to a pressure of 0.99 bar at 273K, 298K and 323K using the Clausius-Clapeyron equation. The CO_2/N_2 selectivities were calculated according to the Ideal Adsorbed Solution Theory (IAST) for CO_2:N_2 mixtures of 0.15:0.85.[S1] The absolute component loadings were fitted either with a single-site Langmuir model or a dual-site Langmuir-Freundlich model, and Wolfram Mathematica was used as the calculation software to solve the equations (coding source from Michael J. Bojdys, a pdf of the manual can be found at www.caferyavuz.com) by following examples from Prof. Hani El-Kaderi's laboratory.[S2, 3]

. CO_2 uptake measurements in moist flue gas conditions were performed on a custom made TPD system at the Korean Research Institute of Chemical Technology. In a typical experiment, 80 mg of sample was pretreated at 150°C for 30 min under pure Helium flow (50 mL/min). Then the flue gas mixture of 81.25% of He, 15% of CO_2 and 3.75% of water was injected at a flow rate of 80 mL/min for 30 minutes and mass change was monitored *in-situ*.

EXPERIMENTAL PROCEDURES

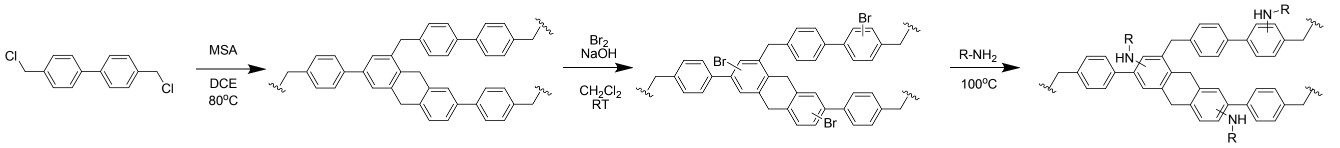

BCMBP **COP-115** **COP-115-A**

COP-115-B R= $C_2H_4NH_2$
COP-115-C R= $C_2H_4NHC_2H_4NH_2$
COP-115-D R= $(C_2H_4NH)_2C_2H_4NH_2$

Scheme S1: Synthesis of **COP-115** series.

Synthesis of COP-115. 4,4'-bis-(chloromethyl)-1,1'-biphenyl (5.34 g, 0.02 mol) was dissolved in dry dichloroethane (30 ml) under argon. Methanesulfonic acid (10.39 mL, 0.16 mol) was slowly added to the solution under vigorous stirring. The mixture was then heated to 80°C and stirred for 24h under argon. After cooling to room temperature, water was added and the precipitate was filtered using vacuum suction. The obtained solid was washed extensively with water, methanol and THF. The obtained yellow powder was dried under vacuum at 100°C for 18h (3.56 g). Elemental analysis: C, 85.94; H, 5.37.

Synthesis of COP-115-A. **COP-115** (3.00 g) and sodium hydroxide (4.30 g, 0.11 mol) were dispersed in dichloromethane (100 mL). Bromine (7 mL, 0.14 mol) in dichloromethane (13 mL) was added and the mixture was stirred for 36h at room temperature. Water was added, the solids filtered off and washed extensively with water, methanol and THF. The obtained solid was dried under vacuum at 100°C for 18h. **COP-115-A** was obtained as a yellow to orange powder (3.46 g). Elemental analysis: C, 73.88; H, 4.36.

General procedure for the amination of COP-115-A. **COP-115-A** (0.45 g) was dispersed in the desired amine (10 mL) and vigorously stirred at 100°C for 72h. The mixture was poured into water, the solids filtered off and washed extensively with water, methanol and THF. The obtained solids were dried at 80°C under vacuum for 18h.

COP-115-B. COP-115-B was obtained from COP-115-A and ethylenediamine as a yellow-orange powder (0.41). Elemental analysis: C, 77.14; H, 5.85; N, 6.15.

COP-115-C. COP-115-C was obtained from COP-115-A and diethylenetriamine as a yellow-orange powder (0.44 g). Elemental analysis: C, 75.94; H, 6.27; N, 7.80.

COP-115-D. COP-115-D was obtained from COP-115-A and triethylenetetraamine as a yellow-orange powder (0.46 g). Elemental analysis: C, 75.97; H, 6.45; N, 8.48.

CHARACTERIZATION:

The polycondensation of the ideal biphenylic monomer, 4,4’-bis-(chloromethyl)-1,1’-biphenyl (BCMBP) with iron(III) chloride was first reported by Wood et al. in 2007.[S4] The resulting polymer showed high surface area of 1874 m^2/g and CO_2 adsorption of 1.7 $mmol.g^{-1}$ at 298K and atmospheric pressure.[S5] There is, however, some dispute over the structure of the obtained network polymer (coded **COP-114**) because of the presence of quinonoids along with aromatic rings, instead of all aromatic with methylene bridges.[S6] We, therefore, employed a second synthetic route for the polycondensation of BCMBP using methanesulfonic acid, also because a "greener" Lewis acid, only to give a less branched **COP-115** devoid of quinonoids (Scheme S1). Methanesulfonic acid has also the advantage of being a liquid, thus easier to handle and remove from the polymer network at the end of the reaction than the hygroscopic iron(III) chloride.[S7, 8] Despite the advantages, it is noteworthy that only a few examples of porous polymer networks have been synthesized using methanesulfonic acid instead of metallic Lewis acids.[S9-11] **COP-115** was obtained in quantitative yields and most importantly, always highly porous.

The elemental composition of COPs were determined by combustion based elemental analysis (Table S1).

Table S1: Elemental analysis of COP-115 complete series.

Porous polymer	C $\%_{weight}$	H $\%_{weight}$	N $\%_{weight}$	Other $\%_{weight}$
COP-115	85.94	5.37	0	8.67
COP-115-A	73.88	4.36	0	21.61
COP-115-B	77.14	5.85	6.15	10.86
COP-115-C	75.94	6.27	7.80	9.99
COP-115-D	75.97	6.45	8.48	9.10

As stated by Wood et al., the ratio between the substituted carbon and unsubstituted carbon resonance can give an information about the crosslinking of the structure.[S4] **COP-115** has a ratio of 1.02, meaning that these structure has a highly rigid structure with almost the same number of substituted and unsubstituted carbon atoms. One advantage of the Davankov type hypercrosslinked polymers is their tolerance to post-synthetic modification because of the rigid, all-hydrocarbon backbone. The post-synthetic modifications often use very harsh conditions (e.g. concentrated nitric acid),which requires the polymer networks to be chemically resistant.[S12-14] Post-synthetic modification of **COP-115** was, therefore, performed with bromine in the presence of sodium hydroxide at ambient conditions (Scheme 2). **COP-115-A** was obtained in quantitative yields. The elemental compositions show a decrease of 13% in carbon content and an increase of the same percentage in other elements, confirming the presence of the high molecular weight bromine atoms in the structures (Table S1). Having the bromine atoms attached to the structure, the last step of post-synthetic modification was the amine tethering, with three different linear ethyleneamines, namely ethylenediamine (EDA), diethylenetriamine (DETA) and triethylenetetraamine (TETA). **COP-115-A** was stirred for three days in the corresponding amines at 100°C to give **COP-115-B,C,D** after repeated washes. Elemental composition of these polymers show significant presence of nitrogen between 4.7 to 8.5%(w/w) indicating the successful tethering of amine groups (Table S1).

FT-IT spectra of **COP-115,A,B** were performed (Figure S4).

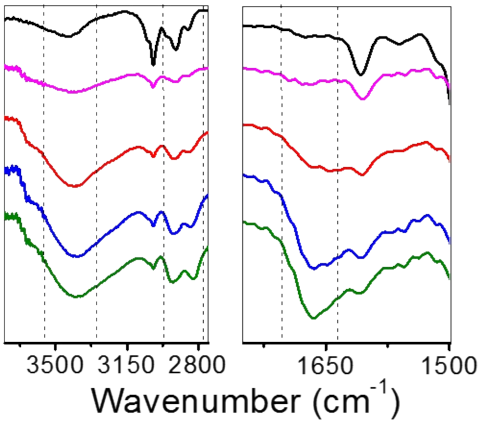

Figure S1: FTIR spectra of **COP-115** series. COP (black), -A (magenta), -B (red), -C (blue), -D (green).

The FTIR spectra (Figure 1) of the aminated COPs show an increase in the intensity of the sp^3 C-H stretch below 3000 cm^{-1} and the appearance of the N-H bend vibration at 1660 cm^{-1}. The broad band around 3400 cm^{-1}is mainly a combination of trapped moisture in the pores and the N-H from primary and secondary amines stretch vibration.

Solid-state ^{13}C Cp-MAS NMR spectra of **COP-115,A,B** were performed in order to characterize further the structures (Figure S4).

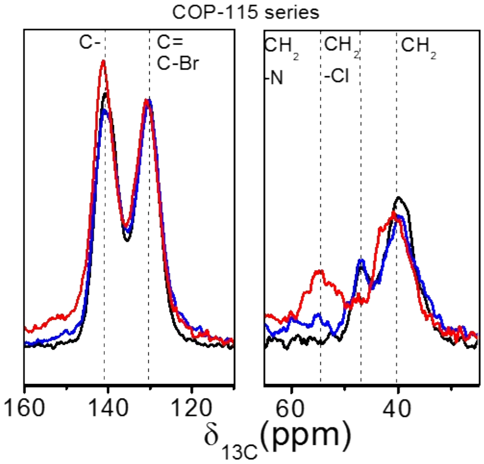

Figure S2. Solid state^{13}C-NMR spectra of **COP-115** (black), **115-A** (blue) and **115-B** (red). Spectra were normalized at 126 ppm to enhance the comparative discussion.

The solid-state ^{13}C Cp-MAS NMR spectra of **COP-115** (Figure S4) present two distinct regions of signals between 150-120 ppm and 35-50 ppm. The two signals at 140 and 126 ppm can be attributed to the resonance of substituted carbon (without H) and to the unsubstituted carbon (with H) of the aromatic and quinonoid units. The signals at 39 ppm can be attributed to the resonance of the alkyl bridges. In **COP-115**, the signal at 46 ppm may be attributed to the leftover chloromethyl units.[S15] After the bromination step, the main difference in the spectra of **COP-115-A** compared to the starting polymer are the relative intensities between the two signals at 140 and 126 ppm. In **COP-115-A**, the intensity of the signal at 126 ppm becomes stronger compared the one at 140 ppm. The alkyl region of the spectra is relatively unchanged, thus indicating that the bromine atoms have mainly reacted with the aromatic and quinonoid fractions. After amination, a new signal appears at 54 ppm corresponding to the alkyl units of the aminated chain. The intensity of the signal at 126 ppm, containing the carbon-bromine signal, diminishes compared to the signal at 140 ppm containing the carbon-nitrogen signal. It can be noted that the signal at 46 ppm also diminishes, indicating that some residual chloromethyls in the structure have reacted with the amine groups.

Thermal stability of all polymer networks was measured through thermogravimetric analysis (Figure S5).

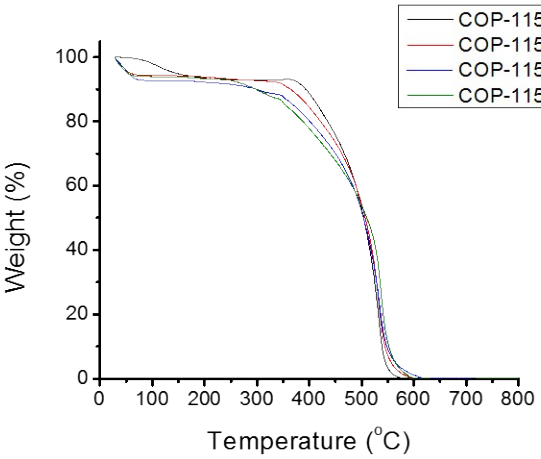

Figure S3. TGA curves of COP-115, A,B,C,D in air.

COP-115 is thermally stable up to 390°C in air. After amine grafting, the thermal stability decreases slightly with longer amine chains, **COP-115-D** being the least stable, up to 315°C. The presence of hydrophilic amine groups in the structure cause the increased loss of moisture before 100°C. All the networks are stable above 300°C in air, which is attributed to the strong covalently linked structure. Thus, degassing at 150°C under high vacuum prior to BET experiments was possible without damaging the structure or losing porosity. The preserved thermal stability is another advantage of grafting amines on the polymer networks as opposed to the physical impregnation of amines.[S16-18]

The sorbent properties were assessed by nitrogen (at 77K) and CO_2 adsorption-desorption isotherms (at 273K, 298K and 323K) (Figure S6).

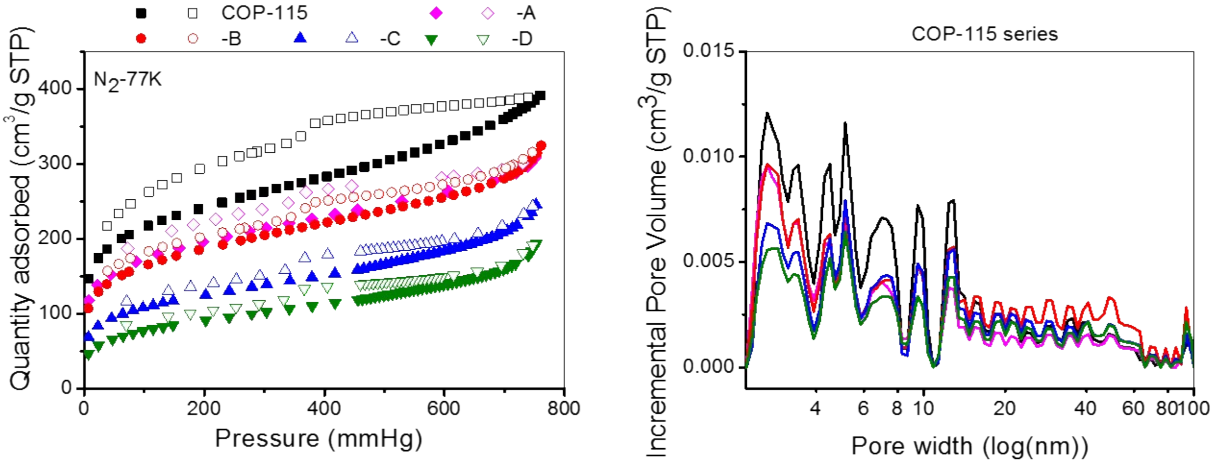

Figure S4. Nitrogen adsorption-desorption isotherms at 77K and NLDFT pore size distribution (single-walled carbon nanotubes model with cylindrical pores) of **COP-115** series.

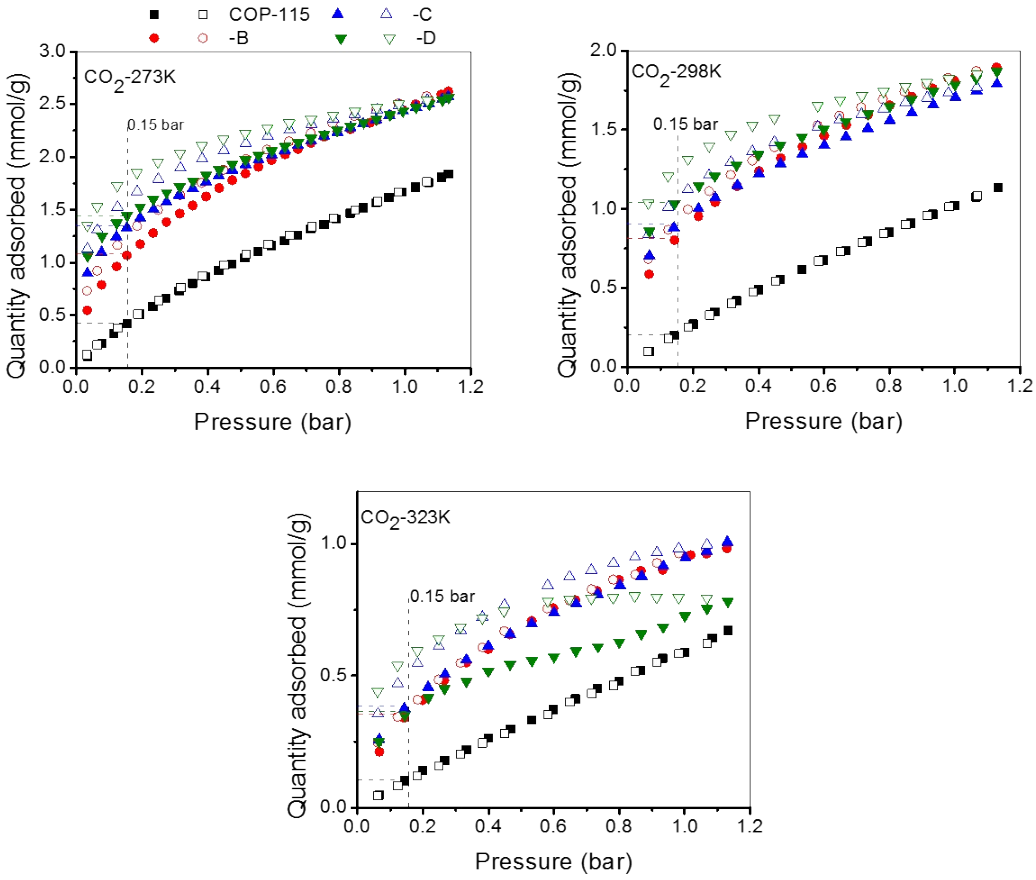

Figure S5. Carbon dioxide adsorption-desorption isotherms of **COP-115** series at 273K, 298K and 323K.

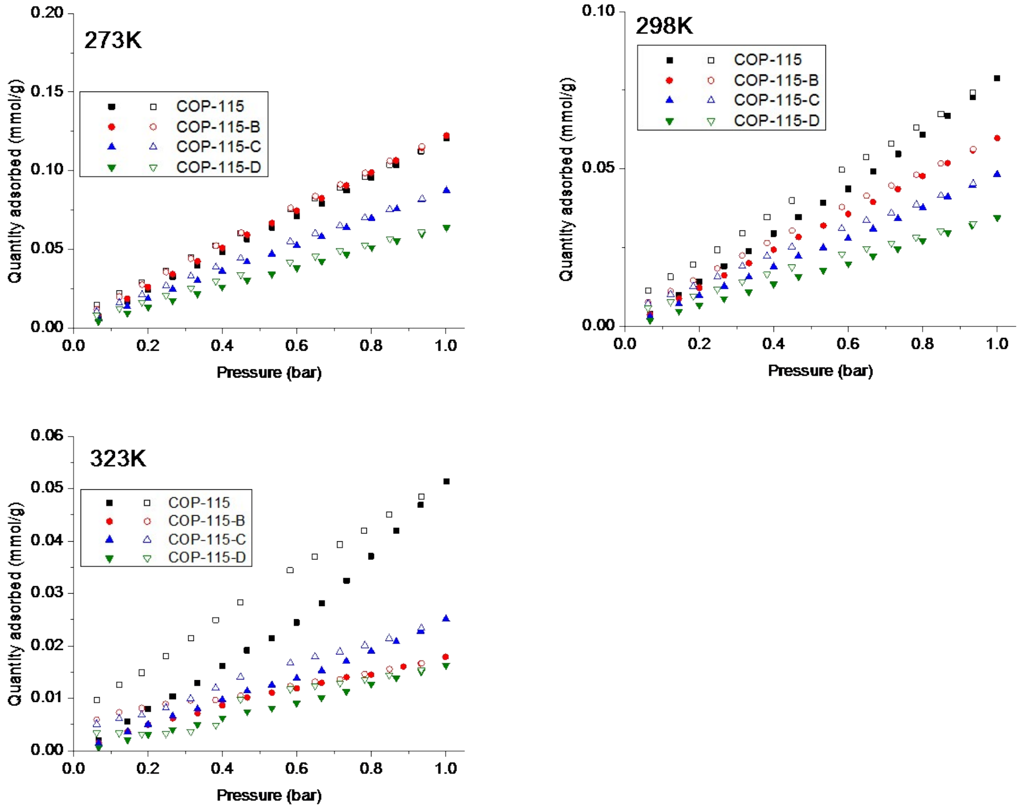

Figure S6: N_2 adsorption-desorption isotherms COP-115 series.

A series of 5 different synthesis of **COP-115** gave surface areas ranging from 608 to 848 m^2/g (TableS2). The chosen network for the post-synthetic modification study has the average surface area of these experiments (735 m^2/g). The NLDFT calculated pore size distributions are ranging from 2.5 to 12.5 nm in width and almost no pores after 40 nm (Figure S6).

Table S2: Textural properties, average experiments.

Compound	Experiment number	BET surface area (m^2/g)
COP-115	1	827
	2	735
	3	665
	4	608
	5	848

Another important feature of an effective CO_2 sorbent is its selectivity towards other gases, especially N_2.[S19] Therefore, we conducted CO_2/N_2 selectivity studies for all the COP networks at 273K, 298K and 323K (Table S3). The CO_2/N_2 selectivities were calculated according to the Ideal Adsorbed Solution Theory (IAST) for CO_2:N_2 mixtures of 0.15:0.85 (dry flue gas conditions).[S1]
Isosteric heats of adsorption were calculated from the adsorption data using Clausius-Clapeyron equation,

$$Q_{st} = R\left[{}^{\partial lnP}\Big/_{\partial\left({}^{1}/_{T}\right)}\right]_{\theta} \quad (1)$$

Where, *R* is the universal gas constant, θ is the fraction of the adsorbed sites at a pressure *P* and Temperature *T*.

Ideal Adsorbed Solution Theory (IAST) [S1, 14]
The calculations for IAST can be derived from the fitting adsorption isotherms with a proper Langmuir model.[1] The absolute component loadings were fitted with either a single-site Langmuir model or a dual-site Langmuir-Freundlich model. Single-site Langmuir model was applied when there were no noticeable isotherm inflections. These models were fitted purely on the basis of giving the best fit with adjusted R^2 values exceeding 0.98. The OriginPro v8.5 was used to solve and calculate the following equations.
The single-site Langmuir model can be defined as,

$$q = \frac{q_{sat}\, b\, p}{1 + b\, p} \quad (2)$$

The dual site Langmuir-Freundlich model can be defined as,

$$q = q_A + q_B = \frac{q_{sat,A}\, b_A\, p}{1 + b_A\, p} + \frac{q_{sat,B}\, b_B\, p}{1 + b_B\, p} \quad (3)$$

Where, *q* is the molar loading of adsorbate; q_{sat} is the saturation loading; *b* is the parameter in the pure component Langmuir adsorption isotherm; *A* and *B* are referring to two different sites.
The IAST selectivities for the CO_2:N_2 (15:85) gas mixtures were calculated using following equation,

$$S = \frac{{}^{q_1}/_{q_2}}{{}^{p_1}/_{p_2}} \quad (4)$$

Where, *S* is the selectivity factor, q_1 and q_2 represent the quantity adsorbed of component 1 and 2, and p_1 and p_2 represent the partial pressure of component 1 and 2.

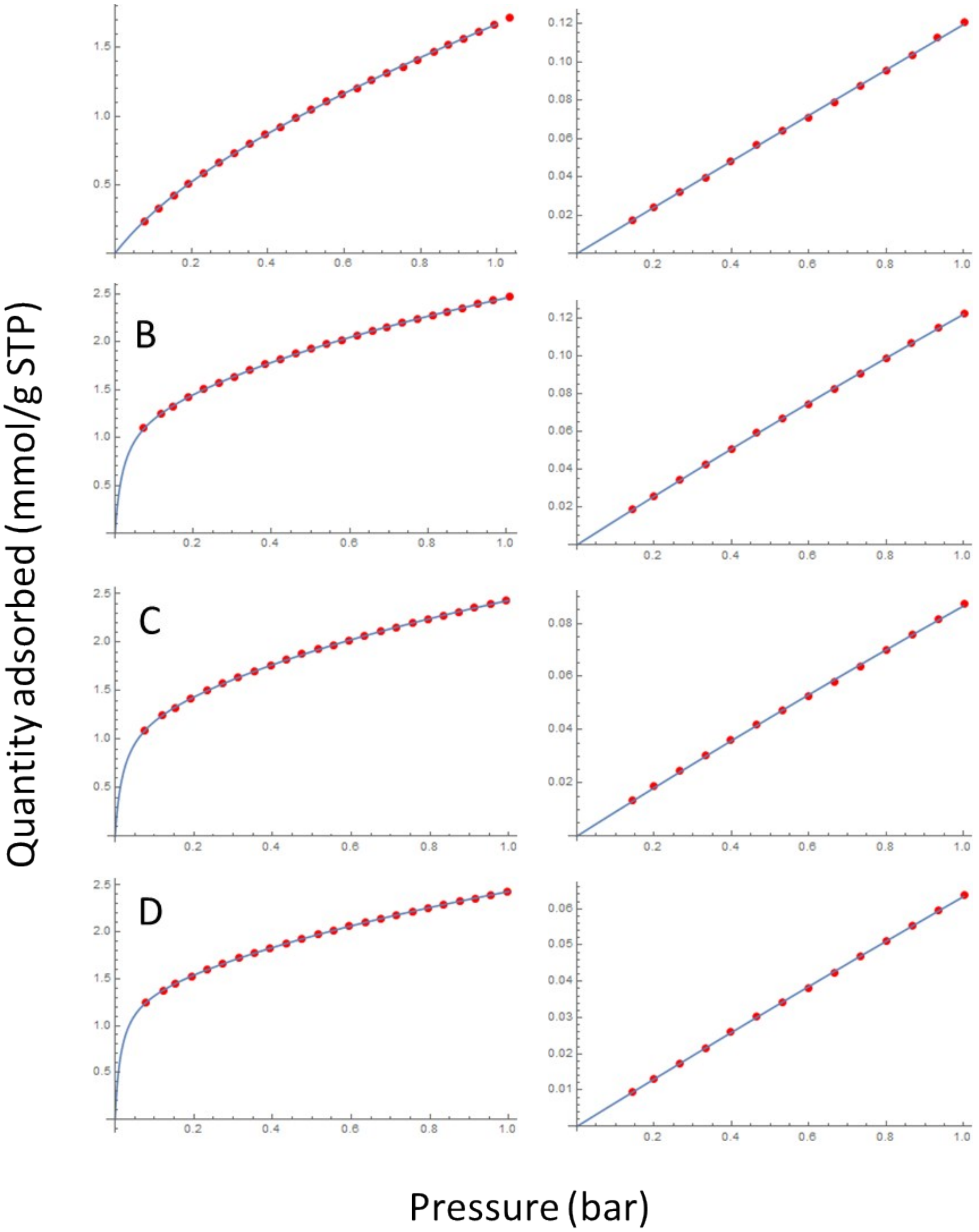

Figure S7. Carbon dioxide (left) and nitrogen adsorption isotherms (right) and the corresponding Langmuir fitted curves of **COP-115** series at 273K.

Table S3: Langmuir Fitting parameters at 273K.

CO_2, 273K	$q_{sat,A}$	b_A	$q_{sat,B}$	b_B
COP-115	0.64332	13.4449	3.5985	0.0950952
COP-115-B	4.09395	0.441694	1.2297	48.7501
COP-115-C	3.97823	0.451598	1.22063	48.6987
COP-115-D	3.71696	0.426924	1.33956	66.9489
N2, 273K				
COP-115	8.12318	0.0149305		

COP-115-B	1.87687	0.0694691		
COP-115-C	1.44394	0.0637244		
COP-115-D	1.72016	0.038253		

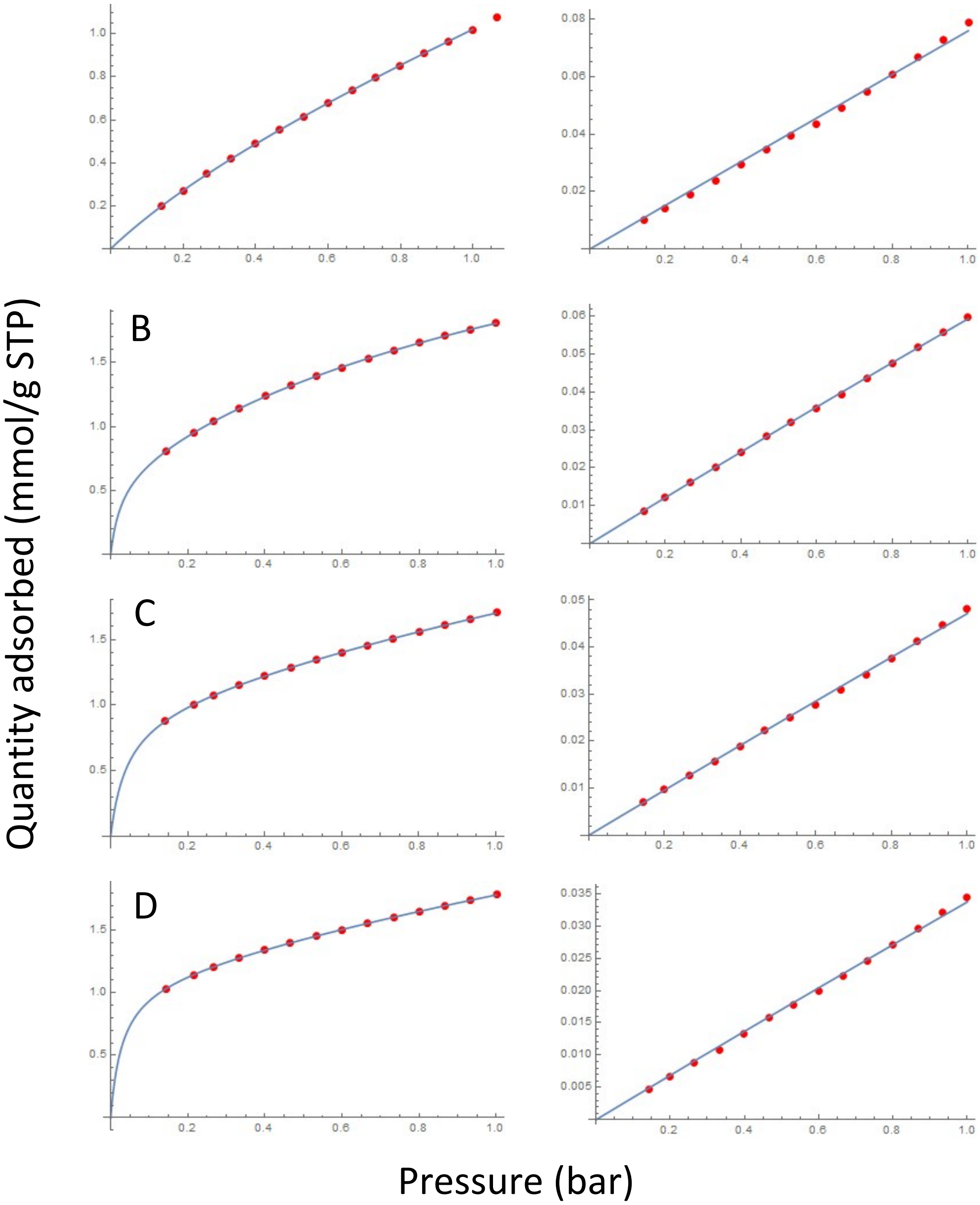

Figure S8. Carbon dioxide (left) and nitrogen adsorption isotherms (right) and the corresponding Langmuir fitted curves of **COP-115** series at 298K

Table S4: Langmuir Fitting parameters at 298K.

CO_2, 298K	$q_{sat,A}$	b_A	$q_{sat,B}$	b_B
COP-115	23.1139	0.0338526	0.390257	2.11023
COP-115-B	2.87716	0.686429	0.655498	35.9263

COP-115-C	4.70514	0.195509	0.970189	23.9094
COP-115-D	4.81444	0.172784	1.10593	33.7377
N2, 298K				
COP-115	18.3955	0.00414617		
COP-115-B	1.79387	0.0342146		
COP-115-C	2.13098	0.0226309		
COP-115-D	1.35172	0.0255694		

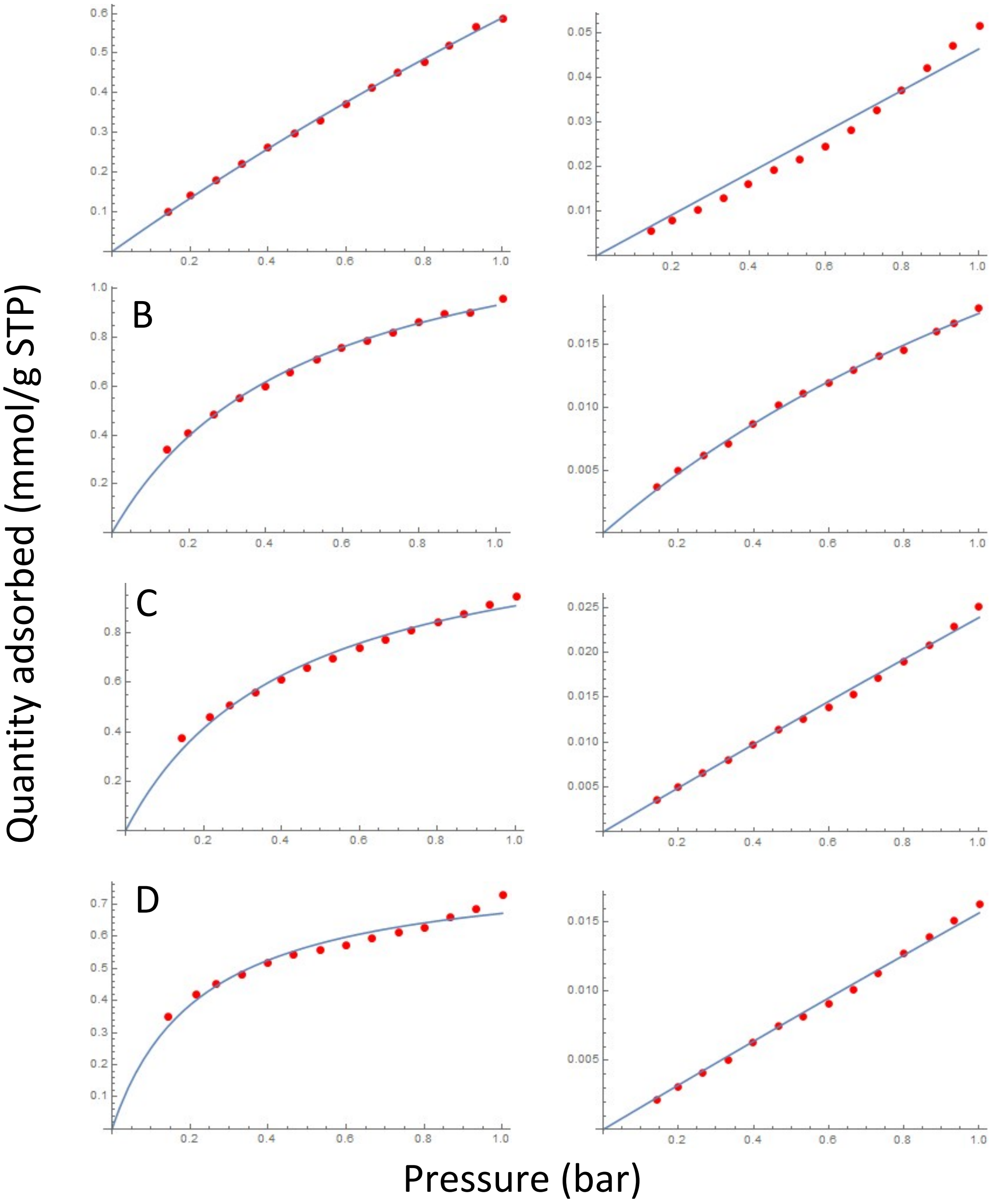

Figure S9. Carbon dioxide (left) and nitrogen adsorption isotherms (right) and the corresponding Langmuir fitted curves of **COP-115** series at 323K

Table S5: Langmuir Fitting parameters at 323K.

CO_2, 323K	$q_{sat,A}$	b_A	$q_{sat,B}$	b_B
COP-115	2.48067	0.219908	2.34015	0.0645385
COP-115-B	0.749488	2.08809	0.659445	1.81058
COP-115-C	0.588415	2.45607	0.710992	2.24301
COP-115-D	0.273698	3.94429	0.549721	4.65705
N2, 323K				
COP-115	15.9475	0.00290865		
COP-115-B	0.0536294	0.483773		
COP-115-C	0.673396	0.0367901		
COP-115-D	0.497809	0.0324974		

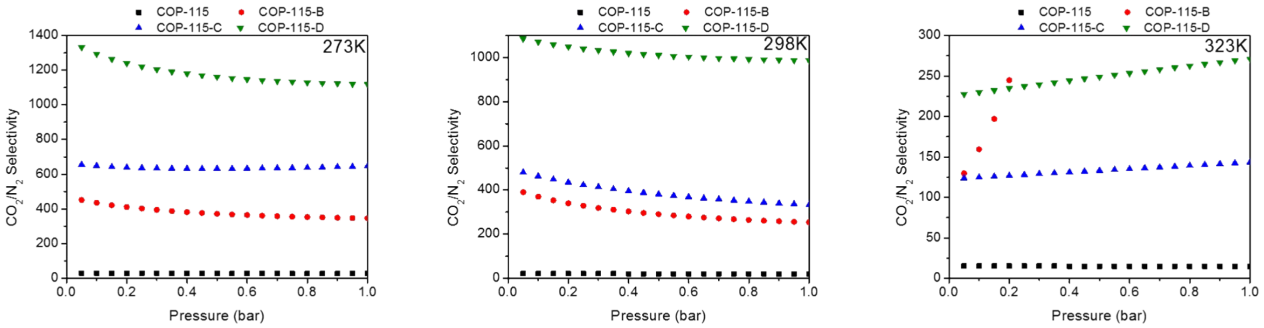

Figure S10. CO_2/N_2 selectivity of **COP-115** (black), **-B** (blue), **-C** (red), **-D** (green) at 273K, 298K and 323K.

Table S6: Heat of adsorption calculation results using different methods

Structure	Qst by Clausius-Clapeyron using 3 temperatures (kJ/mol)	Qst by 3Flex©software using 2 temperatures (kJ/mol)	Qst by 3Flex©software using 3 temperatures (kJ/mol)
COP-115	26.4	21.2	23.2
COP-115-B	35.9	34.2	33.6
COP-115-C	52.7	39.5	67.4
COP-115-D	66.1	39.7	-

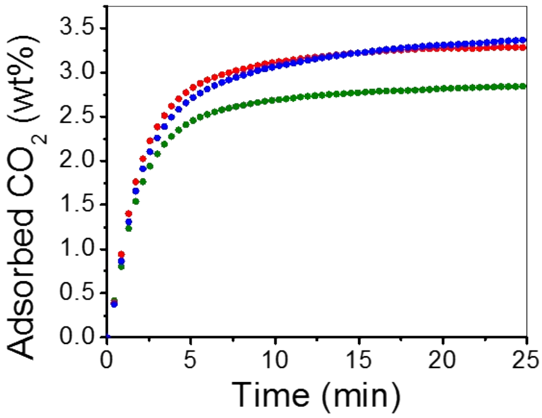

Figure S11. CO_2 uptake under simulated moist flue gas conditions at 40°C of **COP-115** series. COP-B (red), -C (blue), -D (green).

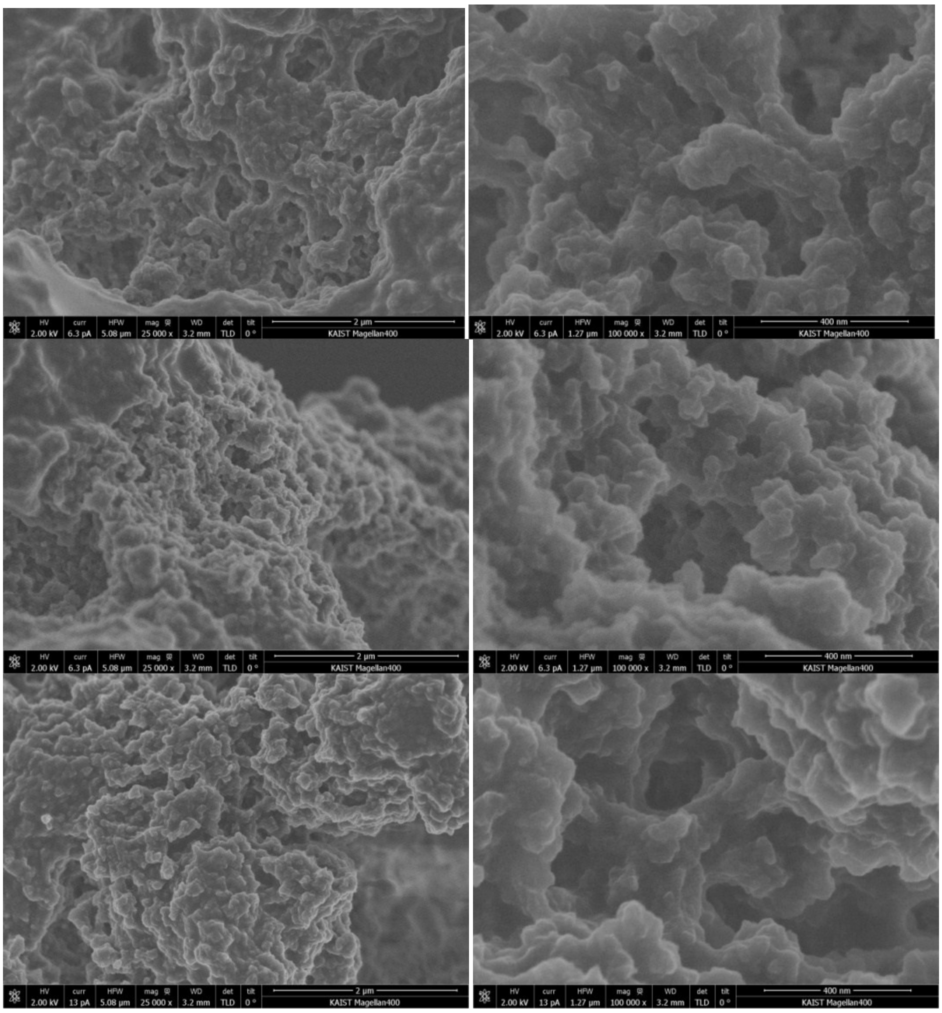

Figure S12: SEM images of COP-115 (top), COP-115-A (middle) and COP-115-B (down) at 2 μm (left) and 400 nm (right) magnification.

References

S1. A. L. Myers and J. M. Prausnitz, *AIChE Journal*, 1965, **11**, 121-127.

S2. P. Arab, E. Parrish, T. Islamoglu and H. M. El-Kaderi, *Journal of Materials Chemistry A*, 2015, **3**, 20586-20594.

S3. B. Ashourirad, A. K. Sekizkardes, S. Altarawneh and H. M. El-Kaderi, *Chemistry of Materials*, 2015, **27**, 1349-1358.

S4. C. D. Wood, B. Tan, A. Trewin, H. Niu, D. Bradshaw, M. J. Rosseinsky, Y. Z. Khimyak, N. L. Campbell, R. Kirk, E. Stöckel and A. I. Cooper, *Chemistry of Materials*, 2007, **19**, 2034-2048.

S5. C. F. Martin, E. Stockel, R. Clowes, D. J. Adams, A. I. Cooper, J. J. Pis, F. Rubiera and C. Pevida, *Journal of Materials Chemistry*, 2011, **21**, 5475-5483.

S6. R. Vinodh, P. Hemalatha, M. Ganesh, M. M. Peng, A. Abidov, M. Palanichamy, W. S. Cha and H.-T. Jang, *RSC Advances*, 2014, **4**, 3668-3674.

S7. M. D. Gernon, M. Wu, T. Buszta and P. Janney, *Green Chemistry*, 1999, **1**, 127-140.

S8. A. Commarieu, W. Hoelderich, J. A. Laffitte and M.-P. Dupont, *Journal of Molecular Catalysis A: Chemical*, 2002, **182**‑**183**, 137-141.

S9. S. Xiong, X. Fu, L. Xiang, G. Yu, J. Guan, Z. Wang, Y. Du, X. Xiong and C. Pan, *Polymer Chemistry*, 2014, **5**, 3424-3431.

S10. R. S. Sprick, A. Thomas and U. Scherf, *Polymer Chemistry*, 2010, **1**, 283-285.

S11. E. Preis, C. Widling, U. Scherf, S. Patil, G. Brunklaus, J. Schmidt and A. Thomas, *Polymer Chemistry*, 2011, **2**, 2186-2189.

S12. T. Islamoglu, M. Gulam Rabbani and H. M. El-Kaderi, *Journal of Materials Chemistry A*, 2013, **1**, 10259-10266.

S13. S. Bernt, V. Guillerm, C. Serre and N. Stock, *Chemical Communications*, 2011, **47**, 2838-2840.

S14. W. Lu, J. P. Sculley, D. Yuan, R. Krishna, Z. Wei and H.-C. Zhou, *Angewandte Chemie International Edition*, 2012, **51**, 7480-7484.

S15. R. V. Law, D. C. Sherrington, C. E. Snape, I. Ando and H. Kurosu, *Macromolecules*, 1996, **29**, 6284-6293.

S16. D. J. Fauth, M. L. Gray, H. W. Pennline, H. M. Krutka, S. Sjostrom and A. M. Ault, *Energy & Fuels*, 2012, **26**, 2483-2496.

S17. Y. Lin, Q. Yan, C. Kong and L. Chen, *Sci. Rep.*, 2013, **3**.

S18. J. C. Hicks, J. H. Drese, D. J. Fauth, M. L. Gray, G. Qi and C. W. Jones, *Journal of the American Chemical Society*, 2008, **130**, 2902-2903.

S19. P. Nugent, Y. Belmabkhout, S. D. Burd, A. J. Cairns, R. Luebke, K. Forrest, T. Pham, S. Ma, B. Space, L. Wojtas, M. Eddaoudi and M. J. Zaworotko, *Nature*, 2013, **495**, 80-84.